Eur. Phys. J. A **8**, 177–185 (2000)

THE EUROPEAN PHYSICAL JOURNAL A

High-spin structure of the neutron-rich $^{104,106,108}_{44}$Ru isotopes: γ-vibrational bands and two-quasiparticle excitations

I. Deloncle[1,a], A. Bauchet[1], M.-G. Porquet[1], M. Girod[2], S. Péru[2], J.-P. Delaroche[2], A. Wilson[1,b], B.J.P. Gall[3], F. Hoellinger[3], N. Schulz[3], E. Gueorguieva[4], A. Minkova[4], T. Kutsarova[5], Ts. Venkova[5], J. Duprat[6], H. Sergolle[6], C. Gautherin[7], R. Lucas[7], A. Astier[8], N. Buforn[8], M. Meyer[8], S. Perriès[8], and N. Redon[8]

[1] CSNSM, IN2P3/CNRS and Université Paris-Sud, 91405 Orsay Campus, France
[2] CEA/DIF, DPTA/SPN, 91680 Bruyères-le-Châtel, France
[3] IReS, IN2P3/CNRS and Université Louis Pasteur, 67037 Strasbourg Cedex 2, France
[4] University of Sofia, Faculty of Physics, 1126 Sofia, Bulgaria
[5] INRNE, BAS, 1784 Sofia, Bulgaria
[6] IPN, IN2P3/CNRS and Université Paris-Sud, 91406 Orsay, France
[7] DAPNIA/SPhN, CEA Saclay, 91191 Gif-sur-Yvette, France
[8] IPNL, IN2P3/CNRS and Université Lyon-1, 69622 Villeurbanne, France

Received: 9 March 2000 / Revised version: 23 May 2000
Communicated by D. Schwalm

Abstract. The ^{104,106,108}Ru nuclei have been produced as fission fragments following the fusion reaction ^{28}Si + ^{176}Yb at 145 MeV bombarding energy; prompt gamma rays emitted in the reaction were detected using the Eurogam II array. Their high-spin level schemes have been obtained, particularly several side bands have been extended or newly observed. Experimental results are discussed in the framework of both collective model and the rotating mean-field approach in which the Gogny force is the sole input. These calculations provide very good descriptions of both low-spin and high-spin structures observed in the neutron-rich even-A Ru isotopes.

PACS. 21.60.Ev Collective models – 21.60.Jz Hartree-Fock approximation – 23.20.Lv Gamma transitions and level energies – 25.85.Ge Charged-particle-induced fission – 27.60.+j $90 \leq A \leq 149$

1 Introduction

The existence of very deformed ground states ($\beta_2 \sim 0.4$) has been well established experimentally in the $A = 100$ mass region for isotopes having $Z \sim 38$–40 (see for instance [1,2]). Many calculations have since attempted to reproduce the sharp shape transition from sphericity to prolate deformation observed when moving from the valley of stability to more neutron-rich nuclei. This is not easily achieved using the standard parameters of various models. For instance, in order to describe equilibrium shapes of several neutron-rich nuclei with $A \sim 100$, the strength of the spin-orbit potential had to be changed as compared to the standard values of the Woods-Saxon potential [3]. Likewise, the shape change is predicted either too early or too late from self-consistent mean-field calculations using the Skyrme effective forces SIII or SkP [4], while it is correctly obtained with the SkM* parametrization [5]. This means that most of the predictions concerning the properties of neutron-rich nuclei with $Z \geq 42$ will be questionable, and therefore it is extremely important that new experimental evidence is obtained in order to validate or reject the various calculations.

Nuclear ground-state masses and deformations have been recently predicted using a macroscopic-microscopic method based on the finite-range droplet model and folded-Yukawa single-particle potentials restricted to axially symmetric shapes [6]. A prolate-to-oblate shape transition is obtained for $N \sim 65$ in all the isotopic series with $Z = 44$ to 48. Because this shape transition is predicted to occur in neutron-rich nuclei, it could not be experimentally verified until recently, when it has been possible to use very efficient Ge detector arrays to study the products of spontaneous and heavy-ion induced fission [7–9]. Such reactions populate relatively high-spin states in neutron-rich nuclei and have proved an efficient means to reach nuclei with a large N/Z ratio. Thus our recent study of the $_{46}$Pd isotopic series has shown that the shape transition predicted at $A = 111$ does not occur [10]. Indeed, studies of the heavier Pd isotopes [11,12] show no evidence for any such transition in isotopes up to and including ^{118}Pd.

[a] e-mail: deloncle@csnsm.in2p3.fr
[b] *Present address:* Department of Physics, University of York, York Y01 5DD UK.

Furthermore, several facts have shown the importance of triaxiality in the mass region with $N \geq 60$ located between the very deformed axially symmetric isotopes having $Z \sim 38$–40 and the spherical $_{50}$Sn isotopes. First of all, analysis of the ratios of reduced electric quadrupole transition probabilities between states in the γ-vibrational bands and in the ground-state bands has pointed out the role of triaxiality in the ground state of even-A neutron-rich $^{108-112}_{44}$Ru isotopes [13]. This feature also comes out from several theoretical predictions of Ru isotopes, either from self-consistent mean-field calculations using Skyrme forces [14,15] or from collective-model calculations of the low-lying collective excitations [16]. Moreover the structure of $^{112-118}_{46}$Pd nuclei has been successfully compared to results of self-consistent microscopic models which give, in those cases, triaxial nuclear shapes [17]. Finally, the high-spin behaviour of $^{107,109}_{45}$Rh nuclei also strongly indicates the importance of including triaxiality in a description of these nuclei [15].

To enlarge our knowledge on the structure of the neutron rich $A = 100$–110 nuclei, we have studied the even-A $^{100-108}_{44}$Ru isotopes, populated as fragments of binary fissions induced by heavy ions [9]. Such a mechanism allows us to populate several high-spin structures in neutron-rich nuclei. Besides the yrast band (which is easily observed up to around spin $16\hbar$), the population of many side bands can be strong enough to allow precise studies to be made, provided that sufficient data are collected corresponding to a specific mass partition. Both collective model and rotating mean-field theory are used for the interpretation of our experimental results. Potential energy surfaces (PESs) have been calculated for $^{100-108}$Ru nuclei through constrained Hartree-Fock-Bogoliubov (HFB) calculations using the D1S Gogny force [18,19]. Since the PESs exhibit shallow minima with triaxial deformation, diagonalization of the complete collective Hamiltonian for quadrupole motion has been performed. This provides information on ground-state bands and positive-parity quadrupole vibrational bands at low excitation energy and spin. On the other hand, kinematic moments of inertia up to high spins (or to high rotational frequencies) are obtained using the cranked HFB theory [20] in which the Gogny force is again the sole input.

2 Experimental procedures and analysis

The $^{100-108}$Ru isotopes have been produced as fission fragments of the polonium isotopes obtained in the fusion reaction ^{28}Si+^{176}Yb at a beam energy of 145 MeV. The beam was provided by the Vivitron accelerator at Strasbourg. A 1.5 mg/cm^2 target of ^{176}Yb was used, onto which a backing of 15 mg/cm^2 Au had been evaporated in order to stop the recoiling nuclei. The prompt γ-rays were detected with the Eurogam II array [21], consisting of 54 escape-suppressed Ge detectors. Thirty of them were large-volume coaxial detectors positioned at backward and forward angles with respect to the beam axis. The remaining 24 detectors, arranged in two rings close to 90° to the beam direction, were four-element "clover" detectors. The data were recorded in an event-by-event mode with the requirement that a minimum of five unsuppressed Ge detectors fired in prompt coincidence. A total of 540 million coincidence events were collected, out of which 135 million were three-fold, 270 million four-fold and 108 million five-fold after off-line suppression.

The off-line analysis consisted of both gated γ-γ matrices and multiple-gated spectra [22]. In addition, we analysed a three-dimensional "cube" built with the software of [23]. The latter technique was useful to make fast inspection of the data, which contain γ-ray cascades emitted by about 130 fission fragments as well as by the nuclei corresponding to the strong fusion-evaporation exit channels [24,25].

The problem of obtaining correct relative intensities, first exposed in ref. [22], has been solved by creating multiple gated spectra directly from data on tapes with the code Fantastic [22]. In fission experiments, spin values can be assigned from angular correlation results [26]. The statistics of our present data was unfortunately too poor to perform such an analysis. Therefore, spin assignments are based upon i) the already known spins of the band-head states [27], ii) the assumption that in yrast decays, spin values increase with excitation energy, and iii) analogy with the level structures of the less neutron-rich Ru isotopes.

3 Experimental results

Many Ru isotopes are populated in the fusion-fission reaction used in this work, from $A = 100$ to $A = 108$. As shown in fig. 1, the Ru isotopes are located in the most produced mass region reached in the reaction and the maximum of

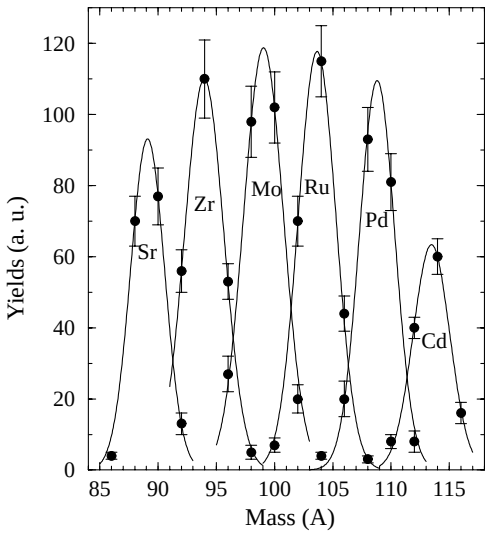

Fig. 1. Yields of the most produced even-even nuclei, obtained as secondary fragments from the fusion reaction ^{28}Si+^{176}Yb at 145 MeV beam energy. They have been normalized to the yields of ^{98,100}Mo and fitted using Gaussian functions.

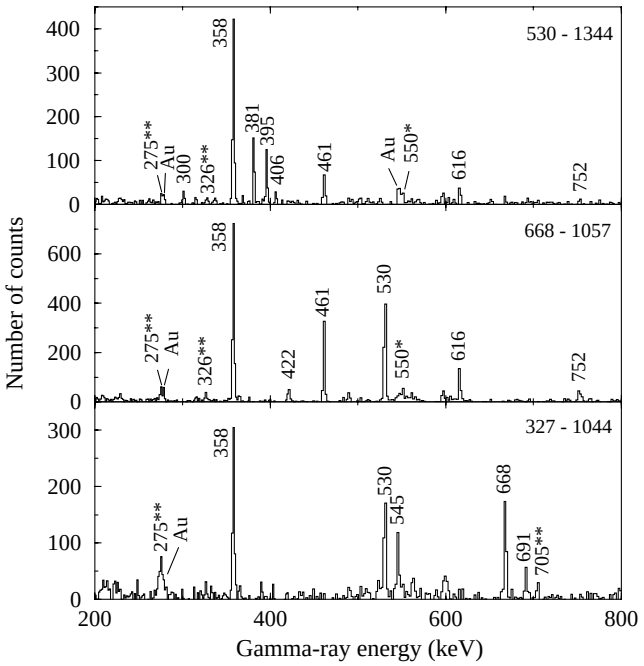

Fig. 2. Spectra of γ-rays in double coincidence with two transitions of ^{104}Ru (their energies are written in the top right corner of each spectrum). The transitions marked with stars belong to the complementary fragments, ^{94}Zr (*) and ^{93}Zr (**).

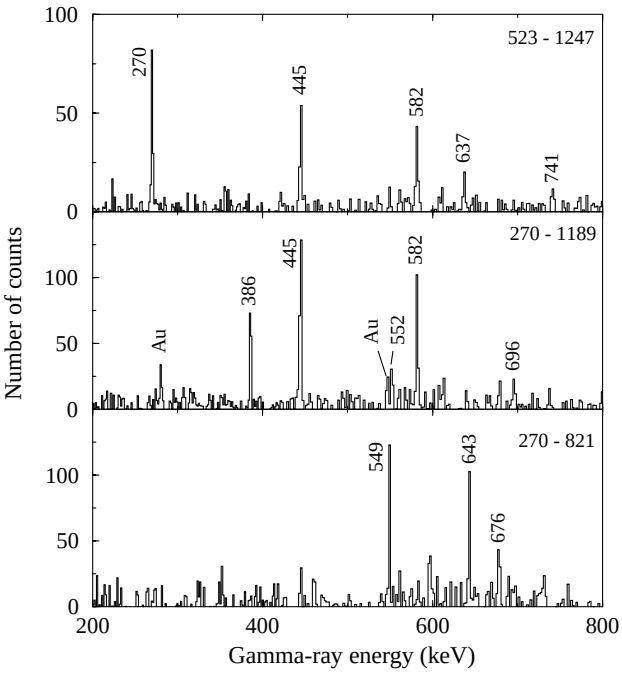

Fig. 3. Spectra of γ-rays in double coincidence with two transitions of ^{106}Ru (their energies are written in the top right corner of each spectrum).

the Ru yields is obtained for $A = 104$ [28]. As prompt γ-rays emitted by complementary fragments are detected in coincidence [2,9], the spectra gated on transitions belonging to Ru isotopes also contain gamma rays associated with Zr nuclei, complementary partners of Ru nuclei in the binary fission of Po.

This work has provided very few new results on high-spin states of ^{100,102}Ru, since they had been extensively studied by means of fusion-evaporation reactions [29–31]: only a new 999 keV transition was added above the (16^+) state of the yrast sequence of ^{102}Ru, allowing us to propose the (18^+) state at 6717 keV excitation energy. On the other hand, the high spin structures of ^{104,106}Ru are now well developed from the analysis of spectra of γ-rays in coincidence with known transitions between low levels. Indeed these nuclei have benefited from the appropriate choice of the fissioning nuclei, as compared to the works using fissions of less neutron-rich Pb compound nuclei [9, 32] in which only the yrast positive-parity bands could be identified. Examples of double-gated spectra showing new transitions depopulating states belonging to negative-parity bands in ^{104}Ru are given in fig. 2. Typical spectra obtained by double-gating on transitions of ^{106}Ru are shown in fig. 3.

The level scheme of ^{104}Ru deduced from the present measurement is shown in fig. 4. It mainly consists of three structures. The yrast positive-parity band, which has been observed up to spin (16^+), is in agreement with previous works [9,33,32], and the decay of the (12^+) state towards the (10^+_2) state at 3284 keV has been identified. The γ-vibrational band is populated: the 751 keV transition decaying the (7^+) state has been added to the structure already known from Coulomb excitation [34]. The third structure, drawn at the left side of fig. 4, comprises several parallel cascades. The most intense is built on the 2232 keV state, which has been determined to have $I^\pi = 5^-$ from Coulomb excitation [34]. This band, already known from a study using deep-inelastic reaction [33], has been extended up to spin (13^-). Even-spin values can be proposed to the states of the cascade built on the new level located at 2600 keV, since such a band is expected in this energy range, as observed in the lighter isotopes [27].

The high-spin level scheme of the neutron-rich ^{106}Ru isotope obtained from this experiment (see fig. 5) looks very similar to that of ^{104}Ru. It has been extended as compared to previous studies since only the positive-parity yrast states were known up to spin (14^+) [9,32] and the first two states of the gamma-vibrational band had been identified from the β-decay of ^{106}Tc [27]. This latter band is now identified up to spin (9^+). Moreover we have observed two new cascades decaying to the 6^+ and 8^+ yrast states, which can form the expected negative-parity bands. There exists no direct connection to the 4^+ yrast state. This implies that, in this reaction, the 5^-_1 state of ^{106}Ru is not populated with enough intensity to be identified. It is worth noting that, already in ^{104}Ru, the out-band decay of the (7^-) state located at 2613 keV is strongly favoured as compared to the in-band decay populating the 5^- state at 2232 keV.

Despite the fact that the yield of ^{108}Ru is very low in this experiment, we have clearly observed the yrast positive-parity band up to spin (12^+), as well as the beginning of a new side band, decaying towards the yrast

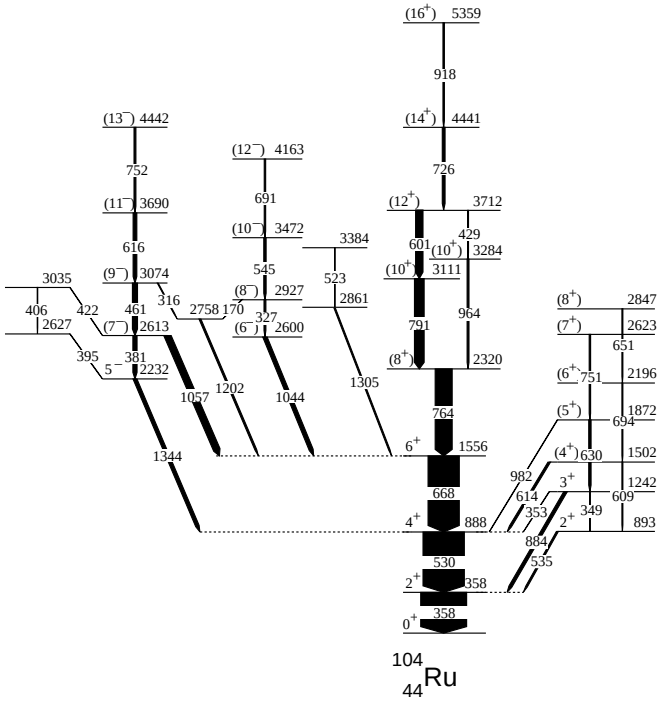

Fig. 4. High-spin level scheme of ^{104}Ru, obtained as a fission fragment in the fusion reaction ^{28}Si+^{176}Yb at 145 MeV beam energy.

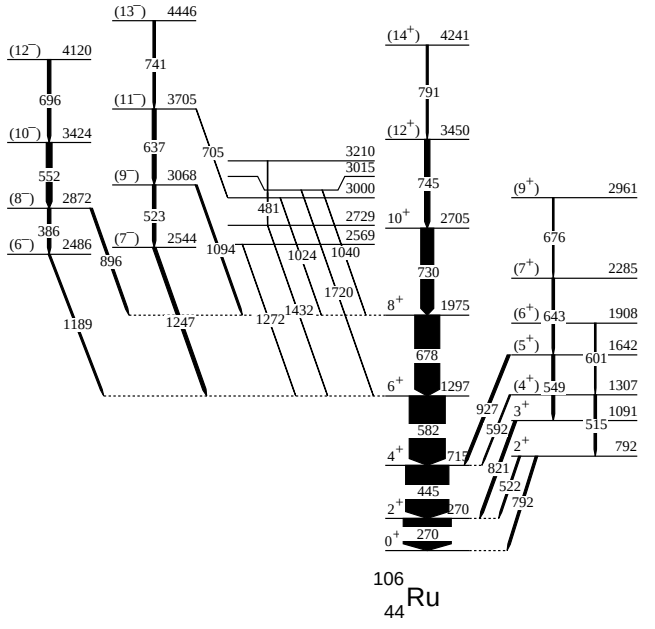

Fig. 5. High-spin level scheme of ^{106}Ru, obtained as a fission fragment in the fusion reaction ^{28}Si+^{176}Yb at 145 MeV beam energy.

positive-parity band by the 1444 and 1231 keV transitions (see fig. 6). From such a decay, negative parity and spin values, 5, 6, and 7, could be proposed for the three new states. It is worth mentioning that the gamma-vibrational band of this nucleus is known up to spin (9^+) from prompt γ-ray spectroscopy after spontaneous fission of ^{248}Cm [13] and ^{252}Cf [35]. This band is very weakly populated in our experiment, up to spin (7^+), as reported in fig. 6.

4 Experimental alignments and structure of the two-quasiparticle bands

The experimental alignments i ($\hbar$) for the yrast positive-parity bands in $^{102-108}$Ru are presented in fig. 7 as functions of rotational frequency. They have been calculated following the procedure described in ref. [36] with the Harris parameters, $\Im_0$=4$\hbar^2$/MeV, $\Im_1$=40$\hbar^4$/MeV^3, which had been obtained in such a way that the alignment plot of ^{102}Ru exhibits flat behaviour after the first alignment [30]. A band crossing is observed around the frequency of 0.35 MeV, with a gain in alignment of 10 $\hbar$. These characteristics have previously been interpreted as a $(\nu h_{11/2})^2$ pair breaking [30]. One observes that before the crossing, the values of alignments are increasing with A, reflecting the known increase of deformation from $N = 58$ to $N = 64$. On the other hand, after the crossing, the values of alignments are closer to each other. This would mean that the broken neutron pair leads the various isotopes to a similar shape.

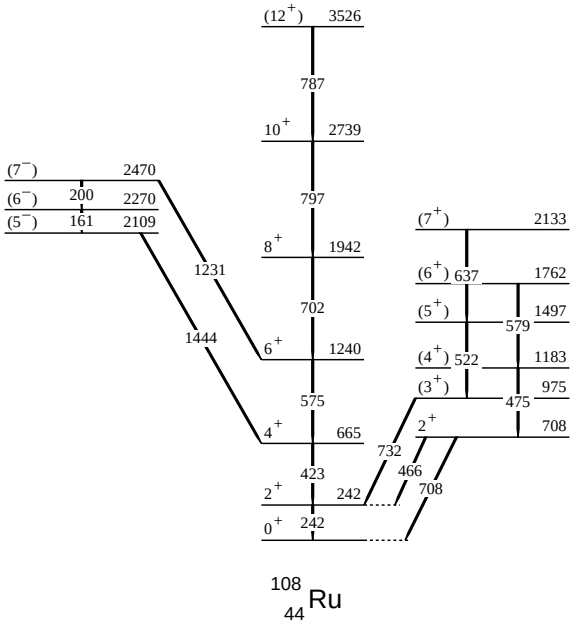

Fig. 6. High-spin level scheme of ^{108}Ru, obtained as a fission fragment in the fusion reaction ^{28}Si+^{176}Yb at 145 MeV beam energy.

Negative-parity side bands are likely to stem from two-neutron configurations: $\nu h_{11/2} \otimes \nu g_{7/2}$ and $\nu h_{11/2} \otimes \nu d_{5/2}$. In this mass region these configurations are known to give rise to semi-decoupled bands, the angular momentum of the $h_{11/2}$ quasineutron being rotation-aligned and that of the positive-parity quasineutron being deformation-aligned. This leads to band heads with lower spins than would be obtained with the maximally aligned configura-

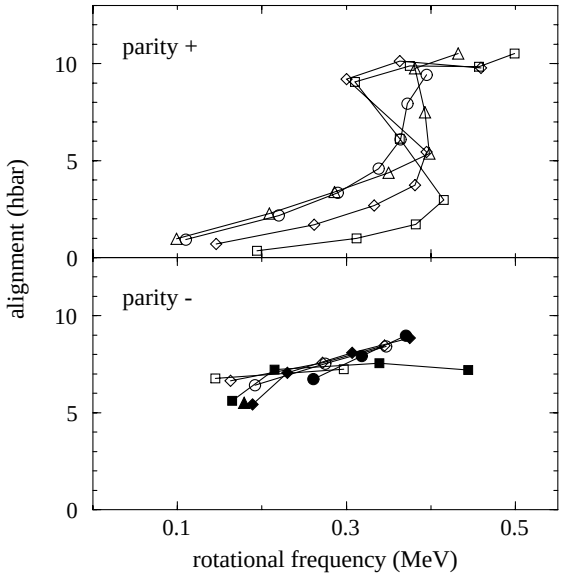

Fig. 7. Experimental alignments for bands in ^{102}Ru (squares, [31] and this work), ^{104}Ru (diamonds), ^{106}Ru (circles), ^{108}Ru (triangles up, [35] and this work). The empty symbols correspond to positive-signature states and the filled symbols to negative-signature states. The values of Harris parameters are $\Im_0 = 4\hbar^2/\text{MeV}$, $\Im_1 = 40\hbar^4/\text{MeV}^3$.

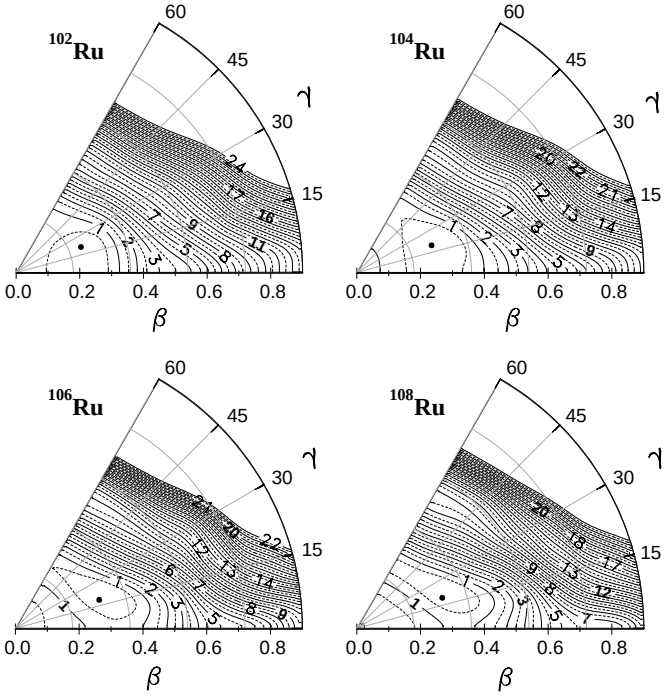

Fig. 8. Potential energy surfaces of ^{102,104,106,108}Ru, obtained via Hartree-Fock-Bogoliubov calculations using the D1S Gogny force. The iso-energy curves are drawn every 0.5 MeV. Some of them are labeled by their energy in MeV. The mean deformation of the ground state is indicated by a dot.

tion, 9^- and 8^-, respectively. The alignments obtained for the negative parity bands of Ru isotopes (shown in fig. 7) are in agreement with such an interpretation: i) the value of initial alignment is around 6 $\hbar$, close to the 5.5 $\hbar$ value expected from a $h_{11/2}$ neutron aligned along the rotational axis, and ii) no crossing is seen near 0.35 MeV in contrast to the yrast positive-parity bands, since one quasineutron blocks the first crossing. Once more, the occupation of the $\nu h_{11/2}$ subshell induces a stabilization of the shape of the different isotopes.

5 Theoretical calculations and discussion

The high-spin level schemes of the $^{102-108}$Ru isotopes are now interpreted in the framework of two separate microscopic models. The first one describes collective motion for the quadrupole coordinates. The collective Hamiltonian, H_{coll}, is built using the Generator Coordinate Method (GCM) and the Gaussian Overlap Approximation (GOA). For more details on this GCM+GOA approach, see ref. [37]. The cranked HFB theory, which describes nuclei in a rotating frame, is used in order to describe the crossings in the yrast positive-parity bands and the two-particle excitation energies. Illustrations of the predictive power of this method are given in ref. [20]. It is worth noting that the sole input of the GCM+GOA and cranked HFB calculations is the D1S Gogny force with the standard parametrization [18,19].

5.1 Potential Energy Surfaces

Figure 8 displays the potential energy surfaces calculated, for the even-A $^{102-108}$Ru isotopes, as functions of the Bohr coordinates, β and γ (the relations giving β and γ as functions of the quadrupole coordinates used in the constrained calculations are those of equations (12) and (13) of ref. [37]). These surfaces include zero-point energies, as discussed in ref. [37]. All of them exhibit a triaxial minimum, characterized by a value of the γ parameter around 25°. The value of the elongation parameter of the minima increases with the neutron number, from 0.2 to 0.3, and the energy of the spherical shape increases by about 1 MeV from ^{102}Ru to ^{108}Ru. Moreover, these surfaces are soft against triaxial deformation, especially for ^{106,108}Ru. This feature excludes the description of these nuclei in terms of axially symmetric shapes.

5.2 Collective Hamiltonian

The collective masses entering H_{coll} are calculated using the perturbation theory given in ref. [38]. As for the three moments of inertia, the so-called Thouless-Valatin dynamical rearrangement contributions [39] have been taken into account. H_{coll} is solved by using basis techniques [40,37], thus providing collective levels and wave functions with vibration and rotation components. From the analysis of these components, it is possible to organize

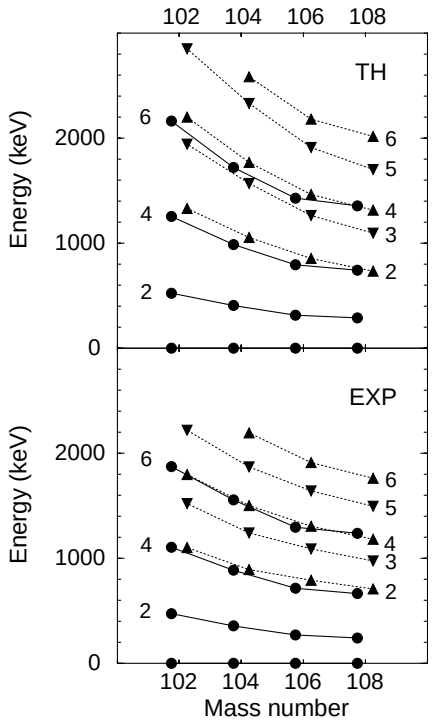

Fig. 9. First excited states of ^{102,104,106,108}Ru: ground-state band (filled circles) and gamma-vibrational band (filled triangles). Comparison of the experimental results and the theoretical results from the resolution of the collective Hamiltonian (see text).

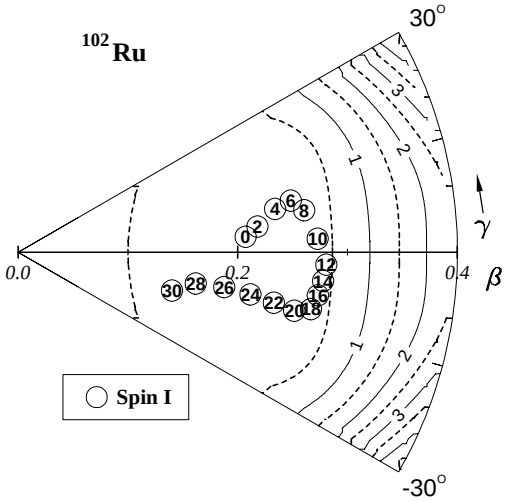

Fig. 10. Calculated shape trajectory for the positive-parity yrast band of ^{102}Ru, for the spin range [0, 30$\hbar$].

the eigenstates into collective bands, ground-state and γ-vibrational band. The solutions for the four isotopes are presented in fig. 9. They show a rather good agreement with the experimental behaviour of the first excited states of the even-even Ru isotopes: the increase of the elongation parameter results in the gradual lowering of all the excited states. The location of the γ-vibrational band at low energy is well calculated. Moreover the staggering in energy observed in the γ-band (the energies of the 4^+ and 6^+ states are depressed in energy as compared to the ones of the odd-spin states) is well reproduced. Such a staggering is due to the softness of the well in the γ direction.

5.3 Description of ground-state bands

Cranked HFB calculations have been performed for the four even-even $^{102-108}$Ru isotopes in order to have a deeper insight into the underlying microscopic structure when the angular velocity increases. In these calculations, the deformation parameters defining the shape of the nucleus are not constrained to keep the value obtained for the PES minimum. While the equilibrium shapes of $^{104-108}$Ru do not vary very much with angular momentum, the case of ^{102}Ru is very spectacular, as illustated in fig. 10. Firstly, the elongation parameter increases from 0.2 to 0.3 when the spin value increases from 0 to 10$\hbar$, and secondly it decreases from 0.3 to 0.13 when the spin value increases from 10 to 30$\hbar$. Simultaneously the asymmetry parameter γ oscillates from positive value when the spin values are lower than 10$\hbar$ to negative value when the spin values are greater than 12$\hbar$. Such a result shows that it is very important not to constrain the shape of nuclei when performing calculations at high spin.

The kinematic moments of inertia of $^{102-108}$Ru have been obtained from the cranked HFB calculations. The calculated values are higher than the experimental results: this systematic difference originates in the absence of the correlation to the vibrational motion which plays a key role in this mass region, as demonstrated by the results presented in the preceding section. Nevertheless in all cases, the first backbending or upbending taking place around 0.35 MeV rotational frequency is due to the alignment of a pair of $h_{11/2}$ neutrons, as mentioned above (sect. 4). As typical examples, the kinematic moments of inertia of ^{102,106}Ru are displayed in fig. 11. The first backbending observed in the yrast band of ^{102}Ru is very well reproduced. Moreover the calculation predicts a second irregularity at 0.5 MeV rotational frequency which is due to the interplay of several concomitant facts: i) the sudden occupation of a proton orbit coming very close to the Fermi level for a rotational frequency $\hbar\omega = 0.5$ MeV; this orbit empties and goes away very rapidly when the rotational frequency increases above 0.5 MeV (this can be considered as a sharp resonance), ii) the gradual disappearance of the proton pairing between $I = 14\hbar$ and $I = 28\hbar$ (see the upper pannel of fig. 11) which gives the global increase of the moment of inertia (from 38 to 45 $\hbar^2$ MeV^{-1}), and iii) the continuous shape change between spin 18 and 28, as shown in fig. 10. It is worth noting that the location of the last experimental point, which is closer in rotational frequency to the point corresponding to the spin value 16$\hbar$ than expected from the extrapolation of the previous points, lends support to the existence of this second anomaly.

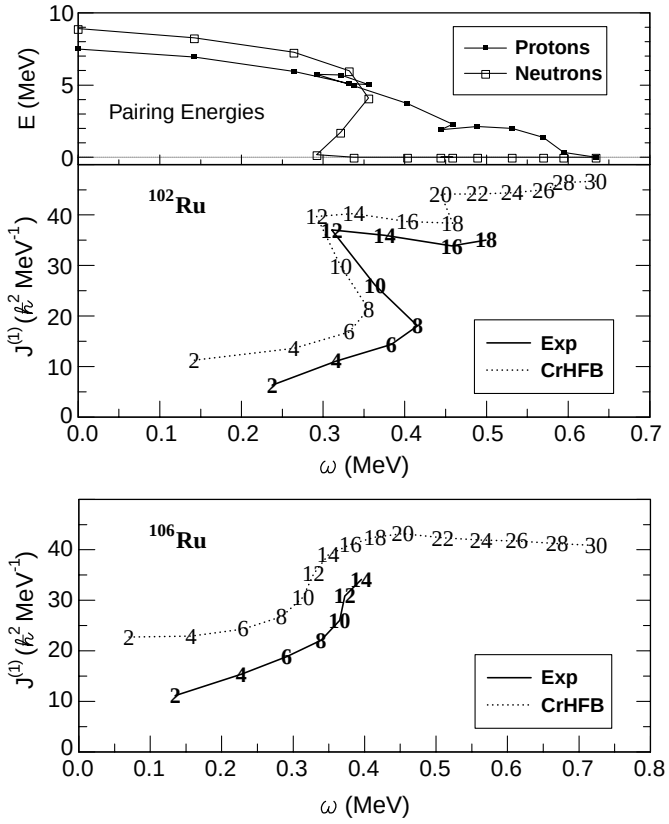

Fig. 11. Cranked Hartree-Fock-Bogoliubov calculations for ^{102,106}Ru: Comparison between theoretical and experimental kinematic moment of inertia as a function of rotational frequency. The spin value of the corresponding excited state is given explicitly. For ^{102}Ru, the calculated values of neutron and proton pairing energies are drawn as functions of rotational frequency.

The description of the first alignment observed in the heavier masses is not as good as in lighter masses (as shown for ^{106}Ru in the bottom pannel of fig. 11). This is due to the greater influence of coupling between the pairing field and the vibrational motion, not included in the present calculations.

5.4 Description of two-quasiparticle states

When using blocking techniques [41], HFB calculations breaking time-reversal symmetry provide information on the two-quasiparticle (qp) states (for each couple of blocked states: equilibrium deformation, energy, ...). The results which have been obtained for $^{100-108}$Ru indicate that the lowest two-proton and two-neutron states are expected at similar excitation energy. The lowest two-proton qp state has $K^\pi = 3^-$, due to the coupling of $\pi 1/2^-[301]$ (from $p_{1/2}$) and $\pi 5/2^+[422]$ (from $g_{9/2}$). Its excitation energy drops with increasing neutron number up to ^{104}Ru and increases for the heavier masses. As for the lowest two-neutron qp states, they are predicted to be also located at an excitation energy around 2 MeV. They involve the low-K orbitals from the $\nu h_{11/2}$ subshell (from $K = 1/2$ in ^{102}Ru to $K = 5/2$ in ^{108}Ru, as expected from the evolution of the neutron Fermi level) coupled to positive-parity orbitals, $K = 3/2^+$ (for the lighter masses) and $5/2^+$ (for the heavier masses), coming from the two $\nu d_{5/2}$ and $\nu g_{7/2}$ spherical subshells.

The predictions concerning the rotational motion built on these two-quasiparticle states obtained with blocking techniques would need a further development, well beyond the calculations performed in this work. Nevertheless, qualitative comparison with the experimental results can be done, showing the quality of the theoretical quasiparticle states located around the Fermi surfaces in these Ru isotopes.

Firstly, the negative-parity band heads observed in this work and discussed in sect. 4 in terms of two-neutron states find their theoretical counterparts. When the neutron number increases, the semi-decoupled bands observed in the lighter masses, evolve towards a strongly coupled structure as the two unpaired neutrons are then predicted to be located in the $5/2^-[532]$ and $5/2^+[413]$ states. The first states of the side band, newly observed in ^{108}Ru (see fig. 6), are in agreement with such a prediction.

Secondly, the two-proton states calculated in the same energy range can be related to other experimental levels. Indeed the first excited state having negative parity in the even-even Ru isotopes are 3^- states; they have been populated in previous studies using β decay [27]. Their energy decreases when the neutron number increases, from $E = 2167$ keV in ^{100}Ru to 1970 keV in ^{104}Ru. Therefore, following theoretical predictions, these 3^- states could originate from two-proton excitations. This would explain why the negative-parity heads of the semi-decoupled band corresponding to the two-neutron excitation do not decay to these 3^- states.

5.5 Prediction of superdeformation in ^{108}Ru

The potential energy surface of ^{108}Ru, shown in fig. 8, exhibits a secondary minimum for very large axial deformation. The potential energy has been calculated as a function of the elongation deformation parameter β, imposing axial symmetry (see the bottom pannel of fig. 12). While the secondary minimum is not very deep, the cranked HFB calculations gives a rotational band with a slowly varying moment of inertia (shown in the upper pannel of fig. 12), from $J^{(1)} \sim 50\hbar^2$ MeV^{-1} at the bottom of the band (spin 2) to $J^{(1)} \sim 55\hbar^2$ MeV^{-1} at the top of the calculated band (spin 20). The value of the mass quadrupole moment of the rotational states is around 20.5 b, leading to a major/minor axis ratio around 1.8, when analyzing the shape in terms of an axial ellipsoid. Taking into account that the excitation energy of the bottom of the SD band above the ground state is of the order of 5 MeV, the SD states are expected to be yrast above $30-36$ $\hbar$.

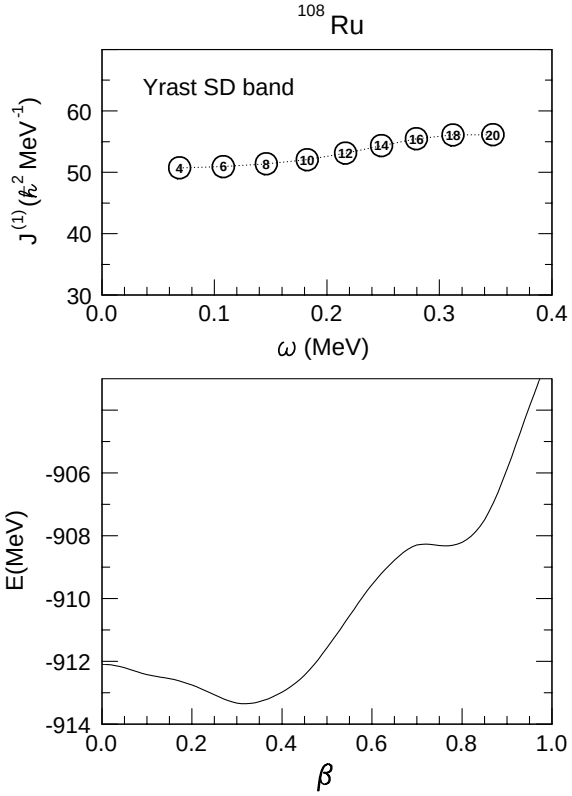

Fig. 12. Bottom: Potential energy of ^{108}Ru, calculated for axial deformation, as a function of the elongation parameter, showing a secondary minimum for large deformation (the zero-point energy is not included in this calculation). Top: Kinematic moment of inertia of the predicted rotational band built in the secondary minimum at large deformation, as a function of rotational frequency.

6 Conclusion

The high efficiency of the new γ-ray detector arrays combined with an original use of a fusion-fission reaction mechanism is a very useful tool for reaching high spin states of some neutron-rich nuclei, which cannot be populated otherwise. In this work, new band stuctures have been identified in the even-even $^{104-108}$Ru, allowing us to discuss the shape evolution in this mass region. The very shallow minima observed in the potential energy surface for non-axial deformation give rise to low-energy gamma-vibrational bands with a characteristic staggering in energy. This means that we cannot rely on predictions obtained for all these nuclei from calculations restricted to axially symmetric shapes. Two self-consistent models, having only one input, the D1S Gogny force with the standard parametrization, have been used to describe, respectively, the low-spin and high-spin structures observed in the even-A $^{102-108}$Ru. These approaches reproduce very well the experimental results, not only in the stability valley (^{102,104}Ru) but also in the neutron-rich isotopes ^{106,108}Ru. Further experimental and theoretical studies of neighbouring nuclei, particularly those having odd-Z numbers, are in progress and will enlarge our understanding of the properties of the neutron-rich nuclei with $A \sim 100$.

The Eurogam project was funded jointly by IN2P3 (France) and the EPSRC (U.K.). We thank the crew of the Vivitron. We are very indebted to A. Meens for preparing the targets, G. Duchêne and D. Prévost for their help during the experiment. This work has been supported in part by the collaboration agreement Bulgarian Academy of Sciences-CNRS under contract No. 2937 and by the Bulgarian National Science Fund under contract No Ph565.

References

1. E. Cheifetz, R.C. Jared, S.G. Thompson, J.B. Wilhelmy, Phys. Rev. Lett. **25**, 38 (1970).
2. M.A.C. Hotchkis et al., Nucl. Phys. A **530**, 111 (1991).
3. J. Skalski, S. Mizutori, W. Nazarewicz, Nucl. Phys. A **617**, 282 (1997).
4. P. Bonche, H. Flocard, P.H. Heenen, S.J. Kreiger, M. Weiss, Nucl. Phys. A **443**, 39 (1985).
5. J. Skalski, P.H. Heenen, P. Bonche, Nucl. Phys. A **559**, 221 (1993).
6. P. Möller, J.R. Nix, W.D. Myers, W.J. Swiatecki, At. Data Nucl. Data Tables **59**, 185 (1995).
7. I. Ahmad, W.R. Phillips, Rep. Prog. Phys. **58**, 1415 (1995).
8. J.H. Hamilton, A.V. Ramayya, S.J. Zhu, G.M. Ter-Akopian, Yu.Ts. Oganessian, J.D. Cole, J.O. Rasmussem, M.A. Stoyer, Prog. Part. Nucl. Phys. **35**, 635 (1995).
9. M.-G. Porquet et al., *Workshop on the High Angular Momentum, Piaski, Poland (August 23-27, 1995)*, Acta Phys. Polonica **27**, 179 (1996).
10. T. Kutsarova et al., Phys. Rev. C **58**, 1966 (1998).
11. M. Houry et al., Eur. Phys. J. A **6**, 43 (1999).
12. R. Krücken et al., Phys. Rev. C **60**, 031302 (1999).
13. J. A. Shannon et al., Phys. Lett. B **336**, 136 (1994).
14. J. Äystö et al., Nucl. Phys. A **515**, 365 (1990).
15. Ts. Venkova et al., Eur. Phys. J. A **6**, 405 (1999).
16. K. Zając, L. Próchniak, K. Pomorski, S.G. Rohoziński, J. Srebrny, Nucl. Phys. A **653**, 71 (1999).
17. M. Houry, Thèse de doctorat de l'Université Paris XI, Orsay (January 2000).
18. J. Dechargé,D. Gogny, Phys. Rev. C **21**, 1568 (1980).
19. J.-F. Berger, M. Girod, D. Gogny, Comput. Phys. Commun. **63**, 365 (1991).
20. M. Girod, J.-P. Delaroche, J.-F. Berger, J. Libert, Phys. Lett. B **325**, 1 (1994).
21. P.J. Nolan, F.A. Beck, D.B. Fossan, Ann. Rev. Nucl. Part. Sci. **44**, 561 (1994).
22. I. Deloncle, M.-G. Porquet, M. Dziri-Marcé, Nucl. Instrum. Methods A **357**, 150 (1995).
23. D.C. Radford, Nucl. Instrum Methods A **361**, 296 (1995).
24. M.-G. Porquet et al., *Proceedings of the International Workshop on Research with Fission Fragments, Benediktbeuern, Germany, 28-30 Oct. 1996* (World Scientific, Singapore 1997) p. 149.
25. M.-G. Porquet et al., *International Symposium on Exotic Nuclear Shapes, Debrecen, Hungary (12-17 May 1997), APH N.S.* Heavy Ions Phys. **7**, 67 (1998).

26. W. Urban et al., Nucl. Instrum. Methods A **365**, 596 (1995).
27. R.B. Firestone, *Table of Isotopes*, 8th edition (Wiley, New York, 1996).
28. M.-G. Porquet et al., *Proceedings of the 2nd International Workshop on Nuclear Fission and Fission Product Spectroscopy, Seyssins, France (April 1998), AIP Conf. Proc.*, Vol. **447**, 212 (1998).
29. M.J.A. De Voigt, J.F.W. Jansen, F. Bruining, Z. Sujkowski, Nucl. Phys. A **270**, 141 (1976).
30. D.R. Haenni, H. Dejbakhsh, R.P. Schmitt, G. Mouchaty, Phys. Rev. C **33**, 1543 (1986).
31. H. Dejbakhsh, S. Bouttchenko, Phys. Rev. C **52**, 1810 (1995).
32. N. Fotiades et al., Phys. Rev. C **58**, 1997 (1998).
33. P.H. Regan et al., Phys. Rev. C **55**, 2305 (1997).
34. J. Stachel et al., Nucl. Phys. A **419**, 589 (1984).
35. Q.H. Lu et al., Phys. Rev. C **52**, 1348 (1995).
36. R. Bengtsson, S. Frauendorf, Nucl. Phys. A **327**, 139 (1979).
37. J. Libert, M. Girod, J.-P. Delaroche, Phys. Rev. C **60**, 054301 (1999).
38. M. Girod, B. Grammaticos, Nucl. Phys. A **330**, 40 (1979).
39. D.J. Thouless, J.G. Valatin, Nucl. Phys. **31**, 211 (1962).
40. K. Kumar, in *Electromagnetic Interaction in Nuclear Spectroscopy* (North-Holland, Amsterdam, 1975) p. 55 (and references therein).
41. S. Péru, Thèse de Doctorat de l'Université Paris VII, Paris (March 1997) and S. Péru et al., to be published.